

Thermal and Structure Analysis Based on Exfoliation of Clay in Thermosensitive Polymer by *in-situ* Polymerization

Marwah Noori Mohammed, Kamal Bin Yusoh*, and Jun Haslinda Binti Haji Shariffuddin

Faculty of Chemical and Natural Resources Engineering, Universiti Malaysia Pahang,
Lebuhraya Tun Razak 26300, Gambang, Pahang, Malaysia

* **Corresponding author:**

tel: +60199339541

email: kamal@ump.edu.my

Received: August 3, 2018

Accepted: December 16, 2018

DOI: 10.22146/ijc.40872

Abstract: Poly(*N*-vinylcaprolactam) (PNVCL) offers superior characteristics as a thermoresponsive polymer for various potential applications. An attractive procedure, namely *in-situ* polymerization, was used to prepare NVCL/clay nanocomposite in different clay ratios. Organo-modified clay as C20 and B30 were employed in a range between 1–5% based on weight. Thermogravimetric analysis (TGA) and Fourier transform infrared spectroscopy (FTIR) were used to study thermal decomposition and to assess bond conversion during polymerization of the nanocomposite. This research was conducted to study PNVCL characteristics with the addition of clay as a nanocomposite. The stretch mode of the carboxylic group (C=O) and (C=C) was present in the band range about $\sim 1635\text{ cm}^{-1}$ for the C20, but it was ranging between $1640\text{ to }1664\text{ cm}^{-1}$ for the B30 of the nanocomposite. It was observed that the decomposition was different for each type of organoclay and the temperature peaked at 30 to 800 °C, to measure the degradation points at 5, 10, and 50%. Comparison results for FTIR and TGA showed that the best nanocomposite was found in the C20 (3%) case.

Keywords: polymer; clay; nanocomposite; thermoresponsive; polymerization; thermal

■ INTRODUCTION

In general, the term stimuli-responsive polymer can be described as the chemical or physical changes of polymer responses to a small external variation in environmental conditions [1-2]. Electric or magnetic scope, mechanical stress, and temperature are physical stimuli that critically affect and mutate molecular interactions. While the change in interaction at the molecular level between polymer chains is a chemical stimulus, which includes ionic factors, chemical agents and pH [3]. Research by the pharmaceutical and biological fields showed that, between all stimuli-responsive polymers, temperature responsive polymers have the most significant attention because most of the diseases that appear due to a change in temperature are vital physiological factors in the body [4-6]. Furthermore, an attractive development was also shown for various applications, such as bioseparation platforms [7], tissue engineering [8], artificial muscles [9-10], environmental issues [11] and sensors [12-13].

Poly(*N*-isopropylacrylamide) (PNIPAM) and poly(*N*-vinylcaprolactam) (PNVCL) are the most popular thermoresponsive polymers due to their lower critical solution temperature (LCST) which is about 33 °C [14-16]. PNVCL is reported to have characteristics such as biotoxicity, biocompatibility, and solubility unlike PNIPAM [17]. The actual interest from the comparison is that PNVCL is more promising for bioanalytical and biomedical applications [18]. When utilized in medical or bio-related applications, the important factors for PNVCL are biocompatibility, macro-porosity, thermal and mechanical properties [19]. For instance, the mechanical characteristics enhancement produces PNVCL that is robust enough for scaffolds of tissue engineering and artificial cartilage [20-21] also, the macrospore structure is able to provide spaces for cell culture [22]. Therefore, it is a great technological significance when the mechanical, macro-porosity and other properties of the PNVCL are developed.

Table 1. Chemicals and materials utilized for the synthesis process

Chemicals	Formula	Purity	Phase	Source
Monomer	C ₈ H ₁₃ NO	98%	S	Aldrich
Initiator	(CH ₃) ₂ C(CN)N=NC(CH ₃) ₂ CN	98%	L	Aldrich
Hexane	C ₆ H ₁₄	99%	L	Aldrich
Diethyl ether	(CH ₃ CH ₂) ₂ O	99.7%	L	Aldrich
Cloisite C20, B30	Material		S powder	Chemical lab
distilled water	H ₂ O	99%	L	Chemical lab
Ammonium hydroxide	NH ₄ OH		L	Merck

It is known that monomer *N*-vinyl caprolactam (NVCL) has poor solubility in aqueous solution; therefore, polymerization usually happens in alcohol/water mixed solution, and small chemical molecules are used for cross-linking [23]. In this scope, Makhaeva et al. [24] synthesized PNVCL, and it was found to have a good thermo-sensitivity and polymerization occurred via methylene bisacrylamide (BIS) as chemical cross-linker in ethyl/water mixed solution. Commonly, PNVCL is chemically cross-linked by BIS characteristic with poor mechanical properties due to variation in reactivity among the cross-linker and the monomer [25].

Imaz and Forcada, Kloxin et al. [4,26] attempted to advance PNVCL mechanical properties by using other cross-linkers such as poly(ethylene glycol) diacrylate (PEGDA) and ethylene glycol dimethacrylate (EGDMA) to produce homogeneous polymeric networks. Schweikl et al. [27] also recently approved the cytotoxicity of both organic chemical cross-linkers. For physical cross-linkers, Loos et al. [28] used silica particles to prepare PNVCL by interacting with the hydrogen bonds between the PVCL carbonyl functions and silica particles in a sol-gel process. However, PNVCL preparation modality cannot stimulate macro-porosity in a polymeric matrix; therefore, silica cross-linked PNVCL nanocomposite has limited applications [29]. Substantially, the fabrication and enhancement of PNVCL properties are still challenging. As mentioned before, the drawback in the previous studies were poor mechanical properties and cytotoxicity for most of the chemical cross-linkers. Therefore, in this work, a novel thermoresponsive polymer PNVCL/clay nanocomposite was prepared by using *in-situ*

polymerization depending on clay nanosheets safety as approved by the cytotoxicity test [30-31].

■ EXPERIMENTAL SECTION

Materials

N-vinyl caprolactam (VCL) was purchased from Sigma Aldrich with a molecular weight of 139.19 g mol⁻¹, while, α,α'-Azobisisobutyronitrile, AIBN (Sigma Aldrich) was used as an initiator. Cloisite C20 and B30 bought from Sigma Aldrich and Hexane (Merck) were used as a solvent. The chemicals and materials employed for synthesis the nanocomposite are represented in Table 1.

Procedure

Preparation of PNVCL/clay nanocomposite

PNVCL/clay nanocomposite investigated in this study was prepared by free-radical polymerization by using clay nanosheets as cross-linking agents. Two kinds of organoclays including C20 (Cloisite®20A, dimethyl dehydrogenated tallow quaternary ammonium (2M2HT)-MMT) and B30 (Cloisite®30B, methyl tallow bis-2-hydroxyethyl quaternary ammonium (MT2EtOH)-MMT). Before synthesis, the clay (C20 or B30) was dried overnight at 70 °C in a ventilated oven to intercalate the clay layers. A magnetic stirrer linked to a condenser was fixed, then the flask was vacuumed. A typical preparation procedure of PNVCL/clay nanocomposite gel can be described as follows: the desired amount of clay (1–5%) was put in a 100 mL three-neck flask mixed with 5 g of NVCL and 30 mL of hexane at 50 °C for 1 h. To start polymerization, the solution was heated at 60 °C then 1 mL of AIBN was dissolved in a 10 mL of hexane and injected into the

solution by using a syringe. After a wash with methanol and water (1:1) to remove the unreacted chemicals, the PNVCL/clay nanocomposite was dried in the vacuum oven to obtain a yellowish gel.

Characterization

To identify the bonding structure between the clay particles (C20 and B30) and monomer in the *in-situ* polymerization, FTIR spectrometer was utilized [32]. Nicolet (Avatar 370 DTGS) was used with a resolution of 4 cm^{-1} from 4000 to 400 cm^{-1} . To increase the signal to noise ratio, each spectrum was taken as an average of 64 scans. TGA measures the amount and rate of change in the weight of a material as a function of temperature or time [5,21,33]. The technique can characterize materials that exhibit weight loss or gain due to decomposition, oxidation or dehydration. Samples curves were plotted with the mass change expressed in percent versus temperature or time. Each sample weighted 10 mg and was heated from 30 to $800\text{ }^{\circ}\text{C}$ at $5\text{ }^{\circ}\text{C}/\text{min}$ under nitrogen.

RESULTS AND DISCUSSION

PNVCL/clay nanocomposite and NVCL were analyzed by using FTIR to detect if polymerization had occurred. From the NVCL monomer spectrum, amide group (C=O) at 1624 cm^{-1} was detected and C–C observed at 1430 cm^{-1} was presented to the aliphatic group in the caprolactam ring. Moreover, a further characteristic of C=C peak appeared at 1648 cm^{-1} and C–H stretching

band was observed at 3108 cm^{-1} in correspondence with studies by Lee et al. and Halligan et al. [8,34].

To ensure polymerization was achieved, i.e., C–H and C=C bands disappeared in the vinyl group of the NVCL monomer; NVCL/C20 (3%) case was investigated. Fig. 1(a) exhibits the NVCL/C20 spectra new peaks that were not typically associated with PNVCL from the literature as the clay was affected. The C–H stretch bond peaks in the range of $2852\text{--}2936\text{ cm}^{-1}$ corresponded to hydroxyl (C–H) group present on the composite surface [35]. The band, centered at $\sim 1635\text{ cm}^{-1}$, represents the stretch mode of the carboxylic group (C=O) [36]. The presence of the above-mentioned carbonyl group indicates that organoclays are chemically linked to the polymer through hydrogen bonding, thereby, forming the polymer/clay nanocomposite. The interaction increases with the increase in the ratio of C20 in NVCL, thus, confirming NVCL/C20 polymerization within the organically modified galleries of Cloisite C20 (Fig. 1(b)).

The vibrations related to hydrogen bonding were observed at a range of $1542\text{--}1686\text{ cm}^{-1}$, found more intense with the increasing percentage of organoclay in the nanocomposites matrix (PNVCL – C20), as compared to neat PNVCL [37]. Furthermore, nanoclay (Cloisite C20) has OH groups on its surface and according to the hypothesis of Ross et al. they might interact with –NCO groups of the isocyanate [38].

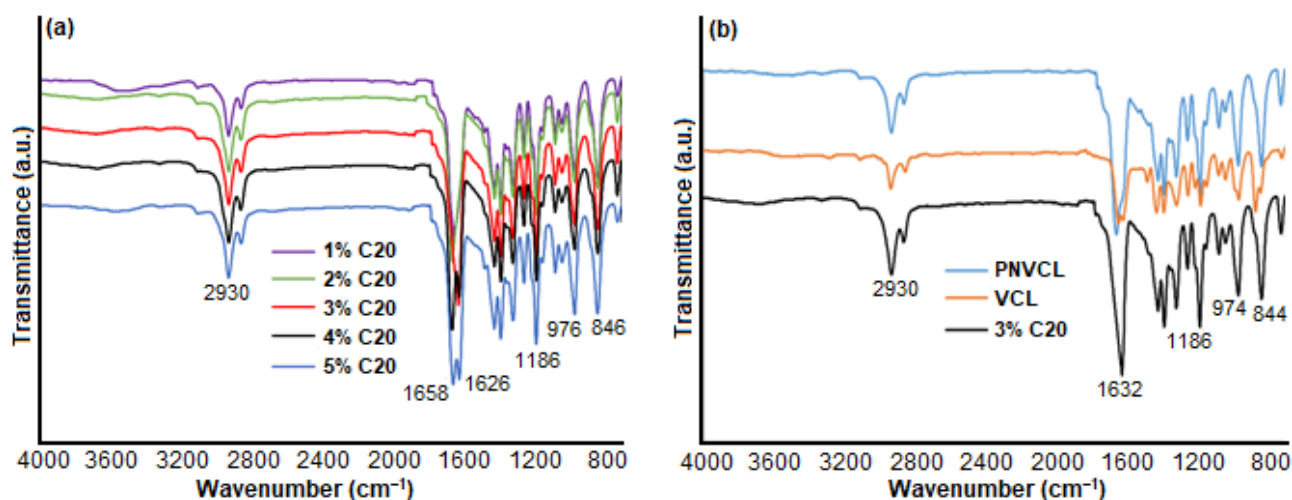


Fig 1. FTIR spectra of: (a) NVCL/C20 (1–5%), (b) PNVCL, NVCL, and NVCL/C20 (3%)

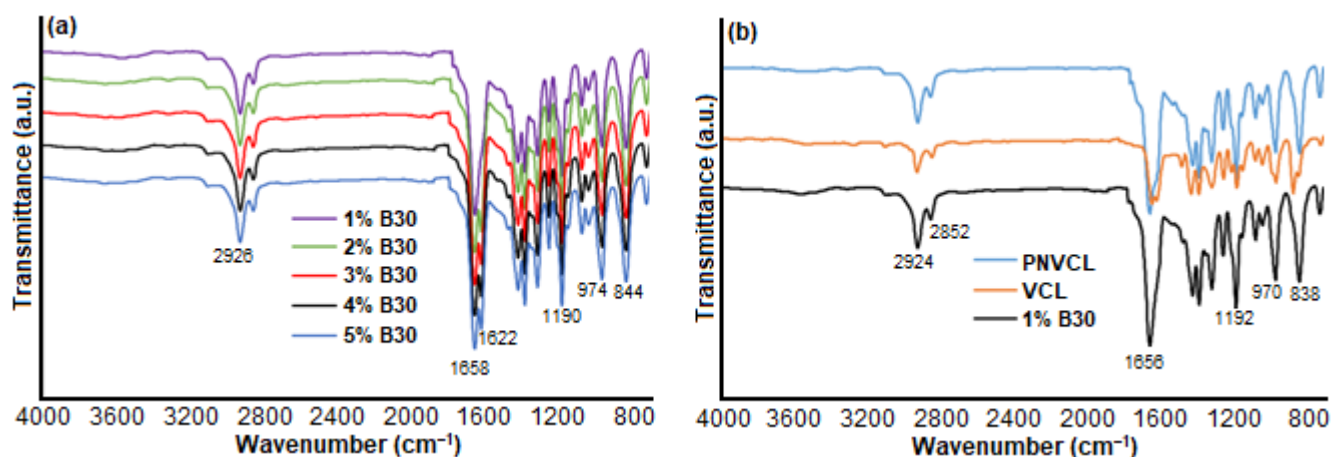


Fig 2. FTIR spectra of: (a) NVCL/B30 (1–5%), (b) PNVCL, VCL, and NVCL/B30 (1%)

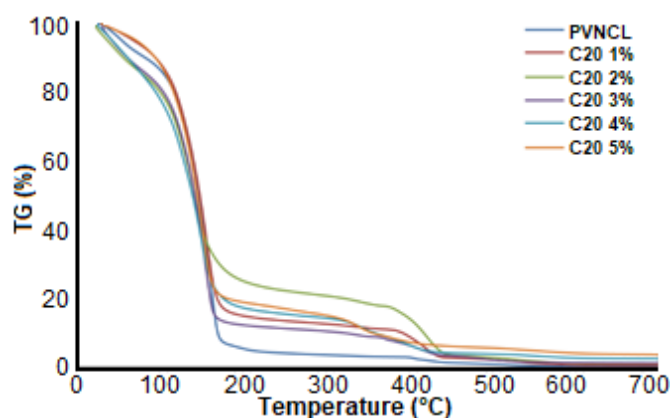


Fig 3. TGA derivative curves for PNVCL and NVCL/C20 (1–5%) nanocomposite

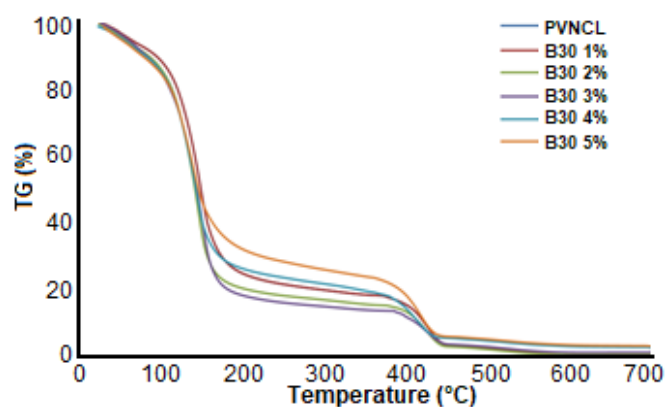


Fig 4. TGA derivative curves for PNVCL and NVCL/B30(1–5%) nanocomposite

B30 effect on the nanocomposite surface based on the FTIR measurements in five ratios are shown in Fig. 2(a). It is clear that the B30 is present in the nanocomposite produced in this study. The C-H stretch band peaks in the range of 2832–2942 cm⁻¹ corresponded to hydroxyl (C-H) group present on the composite surface. The stretch mode of the carboxylic group (C=O) and (C=C) was present in the band range between 1640 to 1664 cm⁻¹ [39]. Fig. 2(b) shows the C=O peak shifting from 1640 cm⁻¹ of NVCL to 1656 cm⁻¹ of NVCL/B30, representing clay intercalation in the nanocomposite. The vibration bands observed for different PNVCL-clays ratios at about wavenumber 1000 to 1100 cm⁻¹ as shown in Fig. 2(a) were due to Si-O stretching and this results corresponding with the study by Sarkar et al. [40].

Results of the TGA weight loss profile of the polymer/clay nanocomposite dried powder samples are shown in Fig. 3 and 4. Organo-modified C20 and B30 were used in this study as a clay. Weight loss occurred when the sample was heated from 30 to 800 °C. The curves in the figures designate the percentage of weight loss with the effect of temperature increase. It can be observed that the weight loss behavior for all samples was huge. Three regions were selected in the TGA pattern for all samples in Fig. 3 and 4. In the first region, the degradation of the mass was very sharp at the temperature range between 100 to 170 °C as shown in Fig. 3 but in Fig. 4 was ranging from 90 to 150 °C. This is due to the loss of the weakly bound OH group and physically adsorbed water from the samples [41].

Table 2. TGA data for PNVCL and nanocomposites under nitrogen flow

Sample	Temperature/°C at mass loss			Residue % at	
	5%	10%	50%	500 °C	600 °C
PNVCL	53.24	81.01	147.14	1.16	0.43
NVCL + 1% (C20)	66.95	93.87	147.80	2.37	0.90
NVCL + 2% (C20)	37.54	56.84	141.88	3.06	1.47
NVCL + 3% (C20)	42.93	61.88	141.94	2.44	1.60
NVCL + 4% (C20)	42.01	60.54	139.08	4.09	2.96
NVCL + 5% (C20)	71.18	94.21	144.72	5.84	4.31
NVCL + 1% (B30)	60.38	92.52	148.66	2.62	0.62
NVCL + 2% (B30)	58.06	86.58	141.57	2.17	0.58
NVCL + 3% (B30)	59.49	82.83	143.97	2.95	1.24
NVCL + 4% (B30)	59.05	86.08	143.19	4.77	3.11
NVCL + 5% (B30)	56.93	82.40	146.16	5.28	3.56

Meanwhile, the degradation of the total weight of the samples ranged from 60 to 95% as shown in Fig. 3, as well as the degradation, was ranging from 56 to 80% as shown in Fig. 4. This behavior appeared in all clay types (C20 and B30). In the second region, the gradual change of weight at a temperature between 170 to 450 °C for C20 and 156 to 400 °C for B30 corresponded to the removal of organic clay residues, interlayer anions and further polymerization of the monomer network [42-43]. The third region showed the lowest weight loss at a temperature above 500 °C due to the strongly bound interlayer anions and removal of the OH group from the sample for both clay types (C20 and B30) as shown in Fig. 3 and 4. The thermograms in Fig. 3 and 4 show that, after an initial loss of 20% of the original weight, there is an almost total rapid degradation of the pure PNVCL and the nanocomposites in the range from 170 to 450 °C. For the decomposition of the nanocomposites around 15–30% is left, probably corresponding to the remaining clay and polymer ashes [42].

Comparison of weight loss through TGA for all nanocomposite samples obtained from polymer/clay polymerization is shown in Table 2. Temperature at weight loss 10 and 50%, and residue at 500 and 600 °C are also presented in Table 2. It can be clearly observed that the percentage of residue increases with the increase in clay ratio from 1 to 5% in the nanocomposite. When the temperature increased to 600 °C, the polymer residue was 0.425%. On the other hand, when C20 clay was used, the

nanocomposite residue ranged from 0.9 to 4.31% based on the increase in clay ratio. The nanocomposite residue increased from 0.618 to 3.560% with the increase of B30 ratio at a temperature of 600 °C. This is ascribed to the continued elimination of strongly bound anions and a small contribution of the OH group.

■ CONCLUSION

In summary, a novel biocompatible thermoresponsive PNVCL-Clay nanocomposite was fabricated, and the successful polymerization conformed to the data via FTIR and TGA. This study allows a much greater understanding of the C20 and B30 intercalation based on the polymer systems that were influenced by the weight ratio. On the basis of the FTIR spectrometer; the shifting of the PNVCL/C20 characteristics and PNVCL/B30 peaks, it can be concluded that the C20 layers intercalation had taken place at NVCL interior more than that of B30. FTIR results confirmed the inclusion of clay in the polymer matrix. Mainly, intercalated composites were obtained. Furthermore, when C20 was used, the NVCL/C20 nanocomposite residue ranged from 0.9 to 4.31% based on the increase in clay ratio per weight. Besides that, the NVCL/B30 residue at a temperature of 600 °C also increased from 0.62 to 3.56% with the increase in ratio. The nanocomposites exhibited improvement in thermal stability as determined by TGA, mainly due to its intercalated structure. TGA data showed that the with

higher clay loadings the depolymerization stage becomes less important, suggesting that the clay affects the mechanism of thermal degradation.

■ ACKNOWLEDGMENTS

The authors would like to be obliged to Universiti Malaysia Pahang for providing laboratory facilities and financial assistance under FRGS research grant (RDU160149) and the internal research funding (RDU150398).

■ REFERENCES

- [1] Strachota, B., Matějka, L., Zhigunov, A., Konefał, R., Spěváček, J., Dybal, J., and Puffr, R., 2015, Poly(*N*-isopropylacrylamide)-clay based hydrogels controlled by the initiating conditions: evolution of structure and gel formation, *Soft Matter*, 11 (48), 9291–9306.
- [2] Francis, R., Gopalan, G.P., Sivadas, A., and Joy, N., 2016, “Properties of Stimuli-Responsive Polymers” in *Biomedical Applications of Polymeric Materials and Composites*, Eds. Francis, R., and Kumar, D.S., Wiley-VCH Verlag GmbH & Co. KGaA, Kottayam, Kerala, India, 187–231.
- [3] Karakasyan, C., Mathos, J., Lack, S., Davy, J., Marquis, M., and Renard, D., 2015, Microfluidics-assisted generation of stimuli-responsive hydrogels based on alginates incorporated with thermo-responsive and amphiphilic polymers as novel biomaterials, *Colloids Surf., B*, 135, 619–629.
- [4] Imaz, A., and Forcada, J., 2010, *N*-vinylcaprolactam-based microgels for biomedical applications, *J. Polym. Sci., Part A: Polym. Chem.*, 48 (5), 1173–1181.
- [5] Mohammed, M.N., Yusoh, K.B., and Shariffuddin, J.H.B.H., 2018, Poly(*N*-vinyl caprolactam) thermo-responsive polymer in novel drug delivery systems: A review, *Mater. Express*, 8 (1), 21–34.
- [6] Wu, W., and Zhou, S., 2013, “Responsive Polymer-Inorganic Hybrid Nanogels for Optical Sensing, Imaging, and Drug Delivery” in *Nanomaterials in Drug Delivery, Imaging, and Tissue Engineering*, Eds. Tiwari, A., and Tiwari, A., Wiley, Hoboken, New Jersey, 263–314.
- [7] Nagase, K., Kobayashi, J., and Okano, T., 2009, Temperature-responsive intelligent interfaces for biomolecular separation and cell sheet engineering, *J. R. Soc. Interface*, 6 (Suppl 3), S293–S309.
- [8] Lee, B., Jiao, A., Yu, S., You, J.B., Kim, D.H., and Im, S.G., 2013, Initiated chemical vapor deposition of thermo-responsive poly(*N*-vinylcaprolactam) thin films for cell sheet engineering, *Acta Biomater.*, 9 (8), 7691–7698.
- [9] Seliktar, D., 2012, Designing cell-compatible hydrogels for biomedical applications, *Science*, 336 (6085), 1124–1128.
- [10] Malhotra, A., Mcinnis, M., Anderson, J., and Zhai, L., 2013, “Stimuli-Responsive Conjugated Polymers: From Electronic Noses to Artificial Muscles” in *Intelligent Stimuli-Responsive Materials*, Eds. Li, Q., Wiley, Hoboken, New Jersey, 423–470.
- [11] Sanna, R., Fortunati, E., Alzari, V., Nuvoli, D., Terenzi, A., Casula, M.F., Kenny, J.M., and Mariani, A., 2013, Poly(*N*-vinylcaprolactam) nanocomposites containing nanocrystalline cellulose: A green approach to thermo-responsive hydrogels, *Cellulose*, 20 (5), 2393–2402.
- [12] Sorber, J., Steiner, G., Schulz, V., Guenther, M., Gerlach, G., Salzer, R., and Arndt, K.F., 2008, Hydrogel-based piezoresistive pH sensors: Investigations using FT-IR attenuated total reflection spectroscopic imaging, *Anal. Chem.*, 80 (8), 2957–2962.
- [13] Granados-Focil, S., 2015, “Stimuli-Responsive Polymers as Active Layers for Sensors” in *Functional Polymer Coatings: Principles, Methods, and Applications*, Eds. Wu, L., and Baghdachi, J., John Wiley & Sons, Inc., Hoboken, New Jersey, 163–196.
- [14] Lau, A.C.W., and Wu, C., 1999, Thermally sensitive and biocompatible poly(*N*-vinylcaprolactam): Synthesis and characterization of high molar mass linear chains, *Macromolecules*, 32 (3), 581–584.
- [15] Maeda, Y., Nakamura, T., and Ikeda, I., 2002, Hydration and phase behavior of poly(*N*-

- vinylcaprolactam) and poly(*N*-vinylpyrrolidone) in water, *Macromolecules*, 35 (1), 217–222.
- [16] Beija, M., Marty, J.D., and Destarac, M., 2011, Thermoresponsive poly(*N*-vinyl caprolactam)-coated gold nanoparticles: Sharp reversible response and easy tenability, *Chem. Commun.*, 47 (10), 2826–2828.
- [17] Cortez-Lemus, N.A., and Licea-Claverie, A., 2016, Poly(*N*-vinylcaprolactam), a comprehensive review on a thermoresponsive polymer becoming popular, *Prog. Polym. Sci.*, 53, 1–51.
- [18] Liu, J., Debuigne, A., Detrembleur, C., and Jérôme, C., 2014, Poly(*N*-vinylcaprolactam): A thermoresponsive macromolecule with promising future in biomedical field, *Adv. Healthcare Mater.*, 3 (12), 1941–1968.
- [19] Imran, A.B., Esaki, K., Gotoh, H., Seki, T., Ito, K., Sakai, Y., and Takeoka, Y., 2014, Extremely stretchable thermosensitive hydrogels by introducing slide-ring polyrotaxane cross-linkers and ionic groups into the polymer network, *Nat. Commun.*, 5, 1–8.
- [20] Sun, J.Y., Zhao, X., Illeperuma, W.R., Chaudhuri, O., Oh, K.H., Mooney, D.J., Vlassak, J.J., and Suo, Z., 2012, Highly stretchable and tough hydrogels, *Nature*, 489 (7414), 133–136.
- [21] Mohammed, M.N., Yusoh, K.B., and Shariffuddin, J.H.B.H., 2016, Methodized depiction of design of experiment for parameters optimization in synthesis of poly(*N*-vinylcaprolactam) thermoresponsive polymers, *Mater. Res. Express*, 3 (12), 125302.
- [22] Murphy, C.M., Haugh, M.G., and O'Brien, F.J., 2010, The effect of mean pore size on cell attachment, proliferation and migration in collagen-glycosaminoglycan scaffolds for bone tissue engineering, *Biomaterials*, 31 (3), 461–466.
- [23] Rao, K.M., Rao, K.S.V.K., and Ha, C.S., 2016, Stimuli responsive poly(vinyl caprolactam) gels for biomedical applications, *Gels*, 2 (1), 6.
- [24] Makhaeva, E.E., Thanh, L.T.M., Starodoubtsev, S.G., and Khokhlov, A.R., 1996, Thermoshinking behavior of poly(vinylcaprolactam) gels in aqueous solution, *Macromol. Chem. Phys.*, 197 (6), 1973–1982.
- [25] Belyaev, A.K., Irschik, H., and Krommer, M., 2016, *Mechanics and Model-based Control of Advanced Engineering Systems*, Springer-Verlag Wien, New Delhi, India, 76.
- [26] Kloxin, A.M., Kloxin, C.J., Bowman, C.N., and Anseth, K.S., 2010, Mechanical properties of cellularly responsive hydrogels and their experimental determination, *Adv. Mater.*, 22 (31), 3484–3494.
- [27] Schweikl, H., Hiller, K.A., Bolay, C., Kreissl, M., Kreismann, W., Nusser, A., Steinhauser, S., Wieczorek, J., Vasold, R., and Schmalz, G., 2005, Cytotoxic and mutagenic effects of dental composite materials, *Biomaterials*, 26 (14), 1713–1719.
- [28] Loos, W., Verbrugghe, S., Goethals, E.J., Du Prez, F.E., Bakeeva, I.V., and Zubov, V.P., 2003, Thermoresponsive organic/inorganic hybrid hydrogels based on poly(*N*-vinylcaprolactam), *Macromol. Chem. Phys.*, 204 (1), 98–103.
- [29] Gomes, M.E., Holtorf, H.L., Reis, R.L., and Mikos, A.G., 2006, Influence of the porosity of starch-based fiber mesh scaffolds on the proliferation and osteogenic differentiation of bone marrow stromal cells cultured in a flow perfusion bioreactor, *Tissue Eng.*, 12 (4), 801–809.
- [30] Gürses, A., 2015, *Introduction to Polymer–Clay Nanocomposites*, CRC Press, Taylor & Francis Group, U.S, 105.
- [31] Alcántara, A.C.S., Darder, M., Aranda, P., Ayral, A., and Ruiz-Hitzky, E., 2016, Bionanocomposites based on polysaccharides and fibrous clays for packaging applications, *J. Appl. Polym. Sci.*, 133 (2), 42362.
- [32] Zhang, T., Yuan, Y., Cui, X., Yin, H., Gu, J., Huang, H., and Shu, J., 2018, Impact of side-chain length on the phase structures of P3ATs and P3AT: PCBM films as revealed by SSNMR and FTIR, *J. Polym. Sci., Part B: Polym. Phys.*, 56 (9), 751–761.
- [33] Lyon, R.E., Safronava, N., and Crowley, S., 2018, Thermal analysis of polymer ignition, *Fire Mater.*, 42 (6), 668–679.
- [34] Halligan, S.C., Dalton, M.B., Murray, K.A., Dong, Y., Wang, W., Lyons, J.G., and Geever, L.M., 2017,

- Synthesis, characterisation and phase transition behaviour of temperature-responsive physically crosslinked poly(*N*-vinylcaprolactam) based polymers for biomedical applications, *Mater. Sci. Eng., C*, 79, 130–139.
- [35] Dimitriou, A., Hale, M.D., and Spear, M.J., 2018, The effect of pH on surface activation of wood polymer composites (WPCs) with hydrogen peroxide for improved adhesion, *Int. J. Adhes. Adhes.*, 85, 44–57.
- [36] Subramani, S., Choi, S.W., Lee, J.Y., and Kim, J.H., 2007, Aqueous dispersion of novel silylated (polyurethane-acrylic hybrid/clay) nanocomposite, *Polymer*, 48 (16), 4691–4703.
- [37] Zhang, J., Wu, Q., Li, M.C., Song, K., Sun, X., Lee, S.Y., and Lei, T., 2017, Thermoresponsive copolymer poly(*N*-vinylcaprolactam) grafted cellulose nanocrystals: Synthesis, structure, and properties, *ACS Sustainable Chem.*, 5 (8), 7439–7447.
- [38] Ross, P., Escobar, G., Sevilla, G., and Quagliano, J., 2017, Micro and nanocomposites of polybutadienebased polyurethane liners with mineral fillers and nanoclay: Thermal and mechanical properties, *Open Chem.*, 15 (1), 46–52.
- [39] Kalaivasan, N., and Syed Shafi, S., 2017, Enhancement of corrosion protection effect in mechanochemically synthesized Polyaniline/MMT clay nanocomposites, *Arabian J. Chem.*, 10 (Suppl. 1), S127–S133.
- [40] Sarkar, S., Datta, S.C., and Biswas, D.R., 2014, Synthesis and characterization of nanoclay–polymer composites from soil clay with respect to their water-holding capacities and nutrient-release behaviour, *J. Appl. Polym. Sci.*, 131 (6), 39951.
- [41] Gun'ko, V.M., Savina, I.N., and Mikhalovsky, S.V., 2017, Properties of water bound in hydrogels, *Gels*, 3 (4), 37.
- [42] Fecchio, B.D., Valandro, S.R., Neumann, M.G., and Cavalheiro, C., 2016, Thermal decomposition of polymer/montmorillonite nanocomposites synthesized in situ on a clay surface, *J. Braz. Chem. Soc.*, 27 (2), 278–284.
- [43] Shahabadi, S.I.S., and Garmabi, H., 2014, Qualitative assessment of nanoclay dispersion using thermogravimetric analysis: A response surface study, *J. Thermoplast. Compos. Mater.*, 27 (4), 498–517.